# A mass-spring analogy for modeling the acoustic behaviour of a metamaterial

Maël Lopez[1], Thomas Dupont[2]
Department of Mechanical Engineering, École de Technologie Supérieure
1100, rue Notre-Dame Ouest, Montréal, QC, H3C 1K3, Canada

Raymond Panneton[3]
Department of Mechanical Engineering, Université de Sherbrooke, CRASH-UdeS
2500 boul. de l'Université, Sherbrooke, Québec, J1K 2R1, Canada

**ABSTRACT**

**Absorbing sound almost completely at specific frequencies with conventional acoustic materials whose thickness is much smaller than the wavelength is a challenge, particularly at low frequencies. For this purpose, acoustic metamaterials are of great interest. The metamaterial studied in this research is called multi-pancake cavities. It is composed of a main pore with a repetition of thin annular cavities (pancake cavities). Previous research has shown that this repetition increases the effective compressibility of the main pore. This increase makes it possible to decrease the effective sound speed in the material and, consequently, the main pore resonance frequencies. At these resonances, the metamaterial presents absorption peaks, the first one can have a wavelength to material thickness ratio of more than dozens of times (subwavelength material). To complete the analysis and prediction of absorption peaks (especially secondary peaks) of these metamaterials, this study proposes to adapt a conventional mass-spring model to this metamaterial. Due to the small cavity length-to-diameter ratios, radial propagation is considered inside the annular cavities. This model shows a good agreement with results obtained by finite element method and impedance tube measurements. Finally, comparisons with previous theoretical approaches are presented and discussed.**

## 1 INTRODUCTION

Acoustic metamaterials are of great interest to handle low frequency problems. Among them, perforated material with dead-end periodic structure presents several absorption peaks for wavelength higher than their thickness [1]–[6]. Leclaire et al. [1] have studied a metamaterial composed of a main pore with periodically spaced side branch resonators. They have shown that the periodic structure is responsible for decreasing the material effective compressibility. This decrease leads to a diminution

[1] mael.lopez.1@ens.etsmtl.ca

[2] thomas.dupont@etsmtl.ca

[3] raymond.panneton@usherbrooke.ca

of the effective celerity and consequently a diminution of the material resonance frequencies. To optimize the acoustic effect, Dupont et al. [4] have replaced side branch resonators by thin annular cavities, called pancake cavities, as shown in Figure 1 (a-b). The very small thickness (compared to the diameter) of the cavity imposes that radial propagation dominates inside [7]. Transfer matrix method (TMM) [4], [8] has been previously used to characterize theoretically such metamaterial. Also to describe this metamaterial more precisely a hybrid model (numerical-TMM) has been developed by Kone et al. [6]. Brooke et al. [9] have proposed a model for the effective properties, density and bulk modulus, in linear and nonlinear (high sound pressure level) regimes.

Here, we proposed a simplified model in order to better understand the acoustic behaviour of the metamaterial and to estimate the resonance frequencies by solving an eigenvalue problem. This model is based on a mass-spring analogy. Mass-spring analogy has already been used to model metamaterials [9]–[11]. Viscous and thermal losses are taken into account in the model by considering effective fluid in the main pore and in the pancake cavity with effective fluid method (Johnson-Champoux-Allard model [12]). Necks (pores between two pancake cavities) are identified by masses and the pancake cavities by springs. The radial propagation in the annular pancake cavity imposes that the stiffness (springs) depends on Hankel functions and thus on the frequency.

## 2 MATERIAL AND MODEL

### 2.1 Material

The studied metamaterial is shown in Figure 1 [4]. It is composed of a repetition of identical neck and thin annular air cavity. The neck thickness is $h_n = 1$ mm and its radius is $r_n = 2$ mm. The cavity thickness is $h_c = 1$ mm and its radius is $r_c = 21$ mm. The sample radius is $R_{sample} = 22.22$ mm and the number of periodic unit cell (PUC) is $N = 15$.

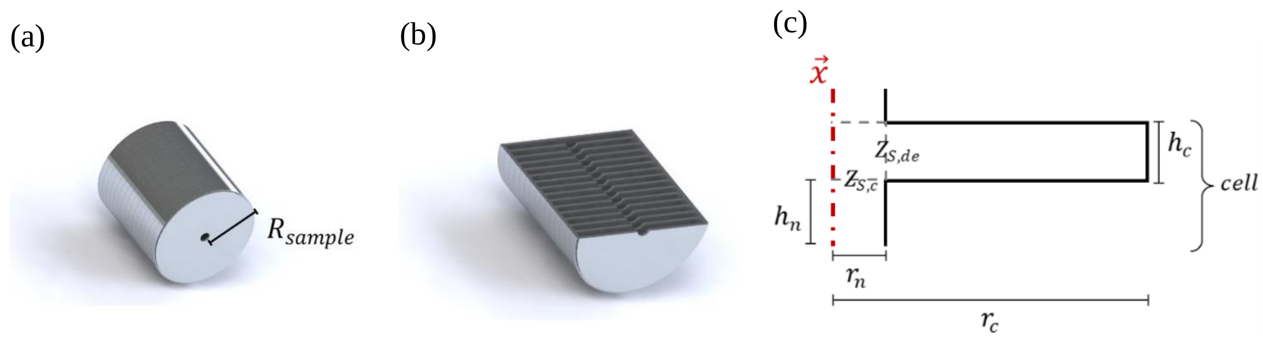


Figure 1 : The metamaterial sample, (a) full, (b) half geometry and (c) a schema of a periodic unit cell (PUC).

### 2.2 Mass-spring model

Due to the periodic arrangement of the cell, a PUC is first studied. The PUC is composed of a neck backed by a pancake cavity. The cavity is here decomposed in two parts, the first one is an annular dead-end volume (for $r \in [r_n\,; r_c]$) and the second one is the junction (for $r \in [0\,; r_n\,]$) as shown in Figure 1 (c).

For the proposed equivalent mass-spring model, each neck is identified by an equivalent mass and each cavity by an equivalent stiffness. The walls are motionless and perfectly reflective to sound. The thermal and viscous losses are considered by effective fluid media for the necks and the annular pancake cavities. Mass and stiffness are then made complex. The Johnson-Champoux-Allard (JCA) parameters are given in TABLE I with necks identified as circular cross-section pores and the annular pancake cavities as slits. The equivalent mass is equal to

$$M = \rho_n A_n h_n, \tag{1}$$

where $\rho_n$ is the neck effective density and $A_n = \pi r_n^2$ the neck cross-section area.

Now by looking at the stiffness, because the cavities are thin, only radial propagation is considered inside the cavity. This implies that the stiffness depends on the frequencies and Hankel functions. The acoustic surface impedance, $Z_{S,de}$, at the interface between the annular dead-end volume and the junction is [7]

$$Z_{S,de} = jZ_{de} \frac{H_0^{(1)}(k_{de}r_n) - H_1^{(1)}(k_{de}r_c)/H_1^{(2)}(k_{de}r_c)H_0^{(2)}(k_{de}r_n)}{H_1^{(1)}(k_{de}r_n) - H_1^{(1)}(k_{de}r_c)/H_1^{(2)}(k_{de}r_c)H_1^{(2)}(k_{de}r_n)}, \tag{2}$$

where $j^2 = -1$, $Z_{de}$ and $k_{de}$ are respectively the effective characteristic impedance and the effective wave number of the annular dead-end pancake cavity given by JCA model [12] for a slit. $H_i^{(m)}$ is the Hankel function of $i$th order and $m$th kind defined as $H_i^{(1)}(x) = J_i(x) + jY_i(x)$ and $H_i^{(2)}(x) = J_i(x) - jY_i(x)$, with $J_i$ and $Y_i$ are Bessel functions of first and second kinds and of $i$th order.

Equation 25 in reference [7] gives the impedance of the pancake cavity at its entrance

$$Z_{S,c} = \frac{1}{j\dfrac{k_0 h_c}{Z_0} + \dfrac{2h_c}{Z_{S,de} r_n}}, \tag{3}$$

where $Z_0$ and $k_0$ are the air characteristic impedance and wave number, respectively.

TABLE I : Effective Johnson-Champoux-Allard parameters of pores and pancake cavities. $\eta$ is the dynamic viscosity of air $(N.s/m^2)$.

| | **Open porosity $\boldsymbol{\phi}$ (1)** | **Tortuosity $\boldsymbol{\alpha_\infty}$ (1)** | **Viscous length $\boldsymbol{\Lambda}$ ($\boldsymbol{m}$)** | **Thermal length $\boldsymbol{\Lambda'}$ ($\boldsymbol{m}$)** | **Static airflow resistivity $\boldsymbol{\sigma}$ ($\boldsymbol{Pa.s/m^2}$)** |
|---|---|---|---|---|---|
| Neck (circular cross-section pore) | 1 | 1 | $r_n$ | $r_n$ | $8\dfrac{\eta}{\phi r_p^2}$ |
| Pancake cavity (slit) | 1 | 1 | $h_c$ | $h_c$ | $12\dfrac{\eta}{\phi h_c^2}$ |

For a one degree of freedom (PUC rigidly backed), combining Hooke's law and Equation 3, the stiffness can be expressed as

$$K = \frac{F_{spring}}{x} = j\omega \frac{PA_n}{v} = j\omega A_n Z_{S,c}, \tag{4}$$

where $F_{spring}$ is the spring force, $x$ is the mass displacement, $\omega$ the angular frequency, $P$ the acoustic pressure at the junction and $v$ the mass velocity ( $v = \dot{x} = j\omega x$ assuming harmonic time dependence of the form $exp(j\omega t)$).

According to Newton's second law and assuming time harmonic dependence, the equation of motion for the studied metamaterial with $N$ repetitions is

$$\left( -\omega^2 \rho_n A_n \begin{bmatrix} h_n' & & & \\ & h_n & & \\ & & \ddots & \\ & & & h_n \end{bmatrix}_{N^2} + \mathrm{k}_c \begin{bmatrix} 1 & -1 & & \\ -1 & 2 & \ddots & \\ & \ddots & \ddots & -1 \\ & & -1 & 2 \end{bmatrix}_{N^2} \right) \mathbf{X} = \begin{Bmatrix} P_1 A_n \\ \\ \\ \end{Bmatrix}, \tag{5}$$

where $\mathbf{X}$ is the mass displacement vector $\mathbf{X} = \{x_1 \quad x_2 \quad \cdots \quad x_n\}^t$, the subscript $t$ refers to the transpose vector. The first term is the diagonal mass matrix, and the second one is the tridiagonal stiffness matrix. $P_1$ is the total pressure applied on the first mass. The first neck thickness is corrected (sample radiation) and equal to $h_n' = h_n + 0.48\sqrt{A_n}(1 - 1.25\, A_n/A_c)$ [13].

Equation 5 can be solved to determine the surface impedance of the metamaterial $Z_{s,MS} = P_1/(j\omega\, x_1)$. Finally, the normal incidence sound absorption coefficient of the rigidly backed metamaterial sample is

$$\alpha_{MS} = 1 - \left| \frac{Z_{s,MS}/\phi_{sample} - Z_0}{Z_{s,MS}/\phi_{sample} + Z_0} \right|^2. \tag{6}$$

with $\phi_{sample} = A_n/A_{sample}$, where $A_{sample} = \pi R_{sample}^2$ is the sample surface.

## 3 Results

The normal incidence sound absorption predicted by the present mass-spring model is shown in Figure 2 (a) for the metamaterial described in section 2.1. The results are compared to those obtained by the TMM approach presented by Kone et al. [8]. To verify both theoretical results, a virtual tube measurement with plane wave at normal incidence on the whole geometry is realized using the Finite Element Method (FEM), on COMSOL Multiphysics, similar as Dupont et al. [4]. COMSOL Multiphysics is used to solve Helmholtz equation with rigid boundary conditions. The thermo-viscous losses are taken into account by assigning effective properties to the air saturating the cavities and necks according to the JCA model and the underlying parameters which are given in TABLE I. As it was observed in reference [4], the different models show several absorption peaks. The mass-spring model and TMM results are almost identical but differs significantly from those of FEM. The difference between the models is the neck modeling. The TMM considers one dimensional acoustic wave propagation, while in the Mass-Spring model a mass behaviour is assumed (constant velocity in the neck). This assumption is still correct because of the thinness of the neck. FEM results predict a first absorption peak nearly equal to one at 357 Hz. Both the TMM and mass-spring model also predict a first absorption peak nearly equal to one, however this time it occurs at 453 Hz (relative error on peak frequency of 27% compared to FEM).

The shift between theoretical models and FEM can be explained because end correction is only added to the first neck (sample radiation in the impedance pipe). However, neck radiation in the pancake cavity should also be considered, which implies additional end correction. Due to the high ratio of length-to-diameter of the cavity, classical formulae [11 12] are not appropriate and predict a correction greater than the cavity thickness. Here, we propose to take the minimum between the classical end correction [13] ($0.48\sqrt{A_n}(1 - 1.25\, A_n/A_c)$ and the half thickness of the cavity. For the sample in this study, the cavity thickness is very thin (pancake cavity), therefore the chosen correction is the half thickness of the cavity. This correction has been applied on both theoretical models. With this new correction, the predicted theoretical sound absorptions are closer to the FEM result – see Figure 2 (b). The theoretical absorption coefficient is 0.97 at 340 Hz (relative error on peak frequency of 4.8% compared to FEM). This comparison shows that the mass-spring model with the proposed end correction describes well the different absorption peaks which are associated with the metamaterial acoustic resonances.

Also, a stopband effect is present around 2 600 Hz [4] and the absorption becomes null. The mass-spring model allows showing that the number of absorption peaks is equal to the number of degrees of freedom and consequently of PUC. Due to high PUC number, the first five peaks are distinct. For the higher ones, they overlap just before the stopband.

One advantage of the mass-spring model compared to the TMM is to estimate the first resonance frequency by solving eigenvalue homogeneous case of Equation 5. Using lossless approximation and low frequency approximation of Hankel functions, the first estimated resonance frequency is equal to 362 Hz. Corresponding to a relative error on the peak frequency of 6% compared to the frequency of the first absorption peak obtained by Equation 6 without approximation.

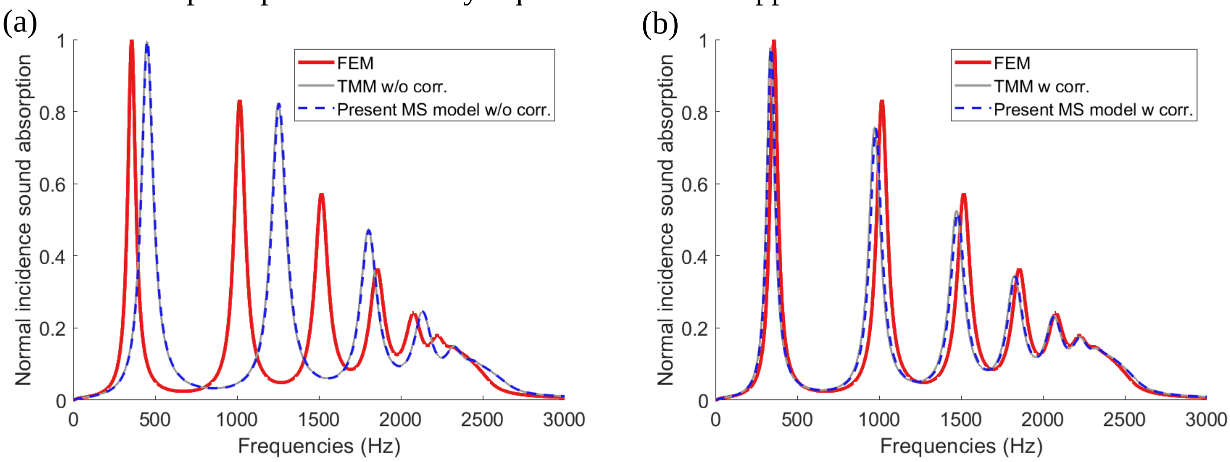


Figure 2 : Normal sound incidence absorption of the multi-pancakes obtained by the Finite Element Method (FEM), the Transfer Matrix Method (TMM) and the proposed Mass-Spring (MS) model. (a) Analytical models without end correction, and (b) with the proposed end correction.

## 4 CONCLUSIONS

A mass-spring model has been developed to describe an acoustic metamaterial composed of periodic array of necks and thin cavities. The model with the neck end correction shows good agreement with finite element method and almost identical results with transfer matrix method. The model has allowed to show that the number of periodic unit cell (i.e., number of degree-of-freedom) determines the number of absorption peaks before the stopband. By using low frequency approximation and lossless case, the model gives a good estimation for the first resonance frequency of the material.

## 5 ACKNOWLEDGEMENTS

This research was supported by the Natural Sciences and Engineering Research Council of Canada (NSERC).

## 6 REFERENCES

[1] P. Leclaire, O. Umnova, T. Dupont, and R. Panneton, "Acoustical properties of air-saturated porous material with periodically distributed dead-end pores," *The Journal of the Acoustical Society of America*, vol. 137, no. 4, pp. 1772–1782, Apr. 2015, doi: 10.1121/1.4916712.

[2] J.-P. Groby, W. Huang, A. Lardeau, and Y. Aurégan, "The use of slow waves to design simple sound absorbing materials," *Journal of Applied Physics*, vol. 117, no. 12, p. 124903, Mar. 2015, doi: 10.1063/1.4915115.

[3] N. Jiménez, W. Huang, V. Romero-García, V. Pagneux, and J.-P. Groby, "Ultra-thin metamaterial for perfect and quasi-omnidirectional sound absorption," *Appl. Phys. Lett.*, vol. 109, no. 12, p. 121902, Sep. 2016, doi: 10.1063/1.4962328.

[4] T. Dupont, P. Leclaire, R. Panneton, and O. Umnova, "A microstructure material design for low frequency sound absorption," *Applied Acoustics*, vol. 136, pp. 86–93, Jul. 2018, doi: 10.1016/j.apacoust.2018.02.016.

[5] V. Romero-García *et al.*, "Perfect Absorption in Mirror-Symmetric Acoustic Metascreens," *Phys. Rev. Applied*, vol. 14, no. 5, p. 054055, Nov. 2020, doi: 10.1103/PhysRevApplied.14.054055.

[6] T. C. Kone, M. Lopez, S. Ghinet, T. Dupont, and R. Panneton, "Thermoviscous-acoustic metamaterials to damp acoustic modes in complex shape geometries at low frequencies," *The Journal of the Acoustical Society of America*, vol. 150, no. 3, pp. 2272–2281, Sep. 2021, doi: 10.1121/10.0006441.

[7] N. S. Dickey and A. Selamet, "Helmholtz resonators: one-dimensional limit for small cavity length-to-diameter ratios," *Journal of Sound and Vibration*, vol. 195, no. 3, pp. 512–517, Aug. 1996, doi: 10.1006/jsvi.1996.0440.

[8] T. C. Kone, S. Ghinet, R. Panneton, T. Dupont, and A. Grewal, "Multi-tonal low frequency noise control for aircraft cabin using Helmholtz resonator with complex cavity," Washington, D.C, Aug. 2021, p. 13.

[9] H. Duan, X. Shen, E. Wang, F. Yang, X. Zhang, and Q. Yin, "Acoustic multi-layer Helmholtz resonance metamaterials with multiple adjustable absorption peaks," *Appl. Phys. Lett.*, vol. 118, no. 24, p. 241904, Jun. 2021, doi: 10.1063/5.0054562.

[10] K. H. Matlack, M. Serra-Garcia, A. Palermo, S. D. Huber, and C. Daraio, "Designing perturbative metamaterials from discrete models," *Nature Mater*, vol. 17, no. 4, Art. no. 4, Apr. 2018, doi: 10.1038/s41563-017-0003-3.

[11] A. L. Vanel, R. V. Craster, and O. Schnitzer, "Asymptotic Modeling of Phononic Box Crystals," *SIAM Journal on Applied Mathematics*, Mar. 2019, doi: 10.1137/18M1209647.

[12] Y. Champoux and J. Allard, "Dynamic tortuosity and bulk modulus in air-saturated porous media," *Journal of Applied Physics*, vol. 70, no. 4, pp. 1975–1979, Aug. 1991, doi: 10.1063/1.349482.

[13] U. Ingard, "On the Theory and Design of Acoustic Resonators," *The Journal of the Acoustical Society of America*, vol. 25, no. 6, pp. 1037–1061, Nov. 1953, doi: 10.1121/1.1907235.

[14] F. C. Karal, "The Analogous Acoustical Impedance for Discontinuities and Constrictions of Circular Cross Section," *The Journal of the Acoustical Society of America*, vol. 25, no. 2, pp. 327–334, Mar. 1953, doi: 10.1121/1.1907041.